

A Hybrid Controller for Obstacle Avoidance in an n -dimensional Euclidean Space

Soulaimane Berkane, Andrea Bisoffi, Dimos V. Dimarogonas

Abstract—For a vehicle moving in an n -dimensional Euclidean space, we present a construction of a hybrid feedback that guarantees both global asymptotic stabilization of a reference position and avoidance of an obstacle corresponding to a bounded spherical region. The proposed hybrid control algorithm switches between two modes of operation: stabilization (motion-to-goal) and avoidance (boundary-following). The geometric construction of the flow and jump sets of the hybrid controller, exploiting a hysteresis region, guarantees robust switching (chattering-free) between stabilization and avoidance. Simulation results illustrate the performance of the proposed hybrid control approach for a 3-dimensional scenario.

I. INTRODUCTION

The obstacle avoidance problem is a long lasting problem that has attracted the attention of the robotics and control communities for decades. In a typical robot navigation scenario, the robot is required to reach a given destination while avoiding to collide with obstacle regions in the workspace. Since the pioneering work by Khatib [1] and the seminal work by Koditscheck and Rimon [2], artificial potential fields and navigation functions have been widely used in the literature, see, e.g., [1]–[4], to deal with the obstacle avoidance problem. The idea is to generate an artificial potential field that renders the goal attractive and the obstacles repulsive. Then, by considering trajectories that navigate along the negative gradient of the potential field, one can ensure that the system will reach the desired target from all initial conditions except from a set of measure zero. This is a well known topological obstruction to *global* asymptotic stabilization by *continuous time-invariant* feedback when the free state space is not diffeomorphic to a Euclidean space, see, e.g., [5, Thm. 2.2]. This topological obstruction occurs then also in the navigation transform [6] and (control)-barrier-function approaches [7]–[10].

To deal with such a limitation, the authors in [11] have proposed a hybrid state feedback controller to achieve robust global asymptotic regulation, in \mathbb{R}^2 , to a target while avoiding an obstacle. This approach has been exploited in [12] to steer a planar vehicle to the source of an unknown but measurable signal while avoiding an obstacle. In [13], a hybrid control law has been proposed to globally asymptotically stabilize a class of linear systems while avoiding an unsafe single point in \mathbb{R}^n .

This research was supported in part by the Swedish Research Council (VR), the European Research Council (ERC) through ERC StG BUCOPHSYS, the Swedish Foundation for Strategic Research (SSF), the EU H2020 Co4Robots project, and the Knut and Alice Wallenberg Foundation (KAW). The authors are with the Division of Decision and Control Systems, KTH Royal Institute of Technology, SE-10044 Stockholm, Sweden. {berkane,bisoffi,dimos}@kth.se

In this work, we propose a hybrid control algorithm for global asymptotic stabilization of a single-integrator system that guarantees the avoidance of a non-point spherical obstacle. Our approach considers trajectories in an n -dimensional Euclidean space and we resort to tools from higher-dimensional geometry [14] to provide a construction of the flow and jump sets where the different modes of operation of the hybrid controller are activated. Our proposed hybrid algorithm employs a hysteresis-based switching between the avoidance controller and the stabilizing controller in order to guarantee forward invariance of the obstacle-free region (related to safety) and global asymptotic stability of the reference position. The parameters of the hybrid controller can be tuned so that the hybrid control law matches the stabilizing controller in arbitrarily large subsets of the obstacle-free region. Preliminaries are in Section II, the problem is formulated in Section III, and our solution is in Sections IV-V, with a numerical exemplification in Section VI.

II. PRELIMINARIES

Throughout the paper, \mathbb{R} denotes the set of real numbers, \mathbb{R}^n is the n -dimensional Euclidean space and \mathbb{S}^n is the n -dimensional unit sphere embedded in \mathbb{R}^{n+1} . The Euclidean norm of $x \in \mathbb{R}^n$ is defined as $\|x\| := \sqrt{x^\top x}$ and the geodesic distance between two points x and y on the sphere \mathbb{S}^n is defined by $d_{\mathbb{S}^n}(x, y) := \arccos(x^\top y)$ for all $x, y \in \mathbb{S}^n$. The closure, interior and boundary of a set $\mathcal{A} \subset \mathbb{R}^n$ are denoted by $\bar{\mathcal{A}}$, \mathcal{A}° and $\partial\mathcal{A}$, respectively. The relative complement of a set $\mathcal{B} \subset \mathbb{R}^n$ with respect to a set \mathcal{A} is denoted by $\mathcal{A} \setminus \mathcal{B}$ and contains the elements of \mathcal{A} which are not in \mathcal{B} . Given a nonzero vector $z \in \mathbb{R}^n \setminus \{0\}$, we define the maps:

$$\pi^\parallel(z) := \frac{zz^\top}{\|z\|^2}, \quad \pi^\perp(z) := I_n - \frac{zz^\top}{\|z\|^2}, \quad \rho^\perp(z) = I_n - 2 \frac{zz^\top}{\|z\|^2} \quad (1)$$

where I_n is the $n \times n$ identity matrix. The map $\pi^\parallel(\cdot)$ is the parallel projection map, $\pi^\perp(\cdot)$ is the orthogonal projection map [14], and $\rho^\perp(\cdot)$ is the reflector map (also called Householder transformation). Consequently, for any $x \in \mathbb{R}^n$, the vector $\pi^\parallel(z)x$ corresponds to the projection of x onto the line generated by z , $\pi^\perp(z)x$ corresponds to the projection of x onto the hyperplane orthogonal to z and $\rho^\perp(z)x$ corresponds to the reflection of x about the hyperplane orthogonal to z . For each $z \in \mathbb{R}^n \setminus \{0\}$, some useful properties of these maps follow:

$$\pi^\parallel(z)z = z, \quad \pi^\perp(z)\pi^\perp(z) = \pi^\perp(z), \quad (2)$$

$$\pi^\perp(z)z = 0, \quad \pi^\parallel(z)\pi^\parallel(z) = \pi^\parallel(z), \quad (3)$$

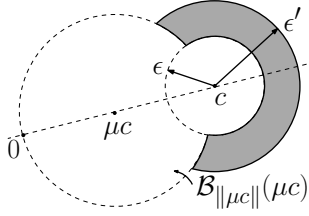


Fig. 1. The helmet region (dark grey) defined in (14).

$$\rho^\perp(z)z = -z, \quad \rho^\perp(z)\rho^\perp(z) = I_n, \quad (4)$$

$$\pi^\perp(z)\pi^\parallel(z) = 0, \quad \pi^\perp(z) + \pi^\parallel(z) = I_n, \quad (5)$$

$$\pi^\parallel(z)\rho^\perp(z) = -\pi^\parallel(z), \quad 2\pi^\perp(z) - \rho^\perp(z) = I_n, \quad (6)$$

$$\pi^\perp(z)\rho^\perp(z) = \pi^\perp(z), \quad 2\pi^\parallel(z) + \rho^\perp(z) = I_n. \quad (7)$$

We define for $z \in \mathbb{R}^n \setminus \{0\}$ and $\theta \in \mathbb{R}$ the parametric map

$$\pi^\theta(z) := \cos^2(\theta)\pi^\perp(z) - \sin^2(\theta)\pi^\parallel(z). \quad (8)$$

In (9)–(14), we define for $v \in \mathbb{R}^n \setminus \{0\}$ some geometric subsets of \mathbb{R}^n , which are described below (14):

$$\mathcal{B}_\epsilon(c) := \{x \in \mathbb{R}^n : \|x - c\| \leq \epsilon\}, \quad (9)$$

$$\mathcal{L}(c, v) := \{x \in \mathbb{R}^n : x = c + \lambda v, \lambda \in \mathbb{R}\}, \quad (10)$$

$$\mathcal{P}^\Delta(c, v) := \{x \in \mathbb{R}^n : v^\top(x - c) \Delta 0\}, \quad (11)$$

$$\begin{aligned} \mathcal{C}^\Delta(c, v, \theta) &:= \{x \in \mathbb{R}^n : (x - c)^\top \pi^\theta(v)(x - c) \Delta 0\} \\ &= \{x \in \mathbb{R}^n : \cos^2(\theta)\|v\|^2\|x - c\|^2 \Delta (v^\top(x - c))^2\} \end{aligned} \quad (12)$$

$$\mathcal{C}_{\nabla}^\Delta(c, v, \theta) := \mathcal{C}^\Delta(c, v, \theta) \cap \mathcal{P}^\nabla(c, v), \quad (13)$$

$$\mathcal{H}(c, \epsilon, \epsilon', \mu) := \overline{\mathcal{B}_{\epsilon'}(c) \setminus \mathcal{B}_\epsilon(c) \setminus \mathcal{B}_{\|\mu c\|}(\mu c)}, \quad (14)$$

where the symbols Δ and ∇ can be selected as $\Delta \in \{=, <, >, \leq, \geq\}$ and $\nabla \in \{<, >, \leq, \geq\}$. The set $\mathcal{B}_\epsilon(c)$ in (9) is the ball centered at $c \in \mathbb{R}^n$ with radius ϵ . The set $\mathcal{L}(c, v)$ in (10) is the 1-dimensional line passing by the point $c \in \mathbb{R}^n$ and with direction parallel to v . The set $\mathcal{P}^\Delta(c, v)$ in (11) is the $(n - 1)$ -dimensional hyperplane that passes through a point $c \in \mathbb{R}^n$ and has normal vector v . The hyperplane $\mathcal{P}^\Delta(c, v)$ divides the Euclidean space \mathbb{R}^n into two closed sets $\mathcal{P}^\geq(c, v)$ and $\mathcal{P}^\leq(c, v)$. The set $\mathcal{C}^\Delta(c, v, \theta)$ in (12) is the right circular cone with vertex at $c \in \mathbb{R}^n$, axis parallel to v and aperture 2θ . The set $\mathcal{C}^\Delta(c, v, \theta)$ in (12) with \leq as Δ (or \geq as Δ , respectively) is the region inside (or outside, respectively) the cone $\mathcal{C}^\Delta(c, v, \theta)$. The plane $\mathcal{P}^\Delta(c, v)$ divides the conic region $\mathcal{C}^\Delta(c, v, \theta)$ into two regions $\mathcal{C}_{\leq}^\Delta(c, v, \theta)$ and $\mathcal{C}_{\geq}^\Delta(c, v, \theta)$ in (13). The set $\mathcal{H}(c, \epsilon, \epsilon', \mu)$ in (14) is called *helmet* and is obtained by removing from the spherical shell (annulus) $\mathcal{B}_{\epsilon'}(c) \setminus \mathcal{B}_\epsilon(c)$ the portion contained in the ball $\mathcal{B}_{\|\mu c\|}(\mu c)$, see Fig. 1. The next geometric fact will be used.

Lemma 1 ([15]): Let $c \in \mathbb{R}^n$ and $v_1, v_2 \in \mathbb{S}^{n-1}$ be some arbitrary unit vectors such that $\mathbf{d}_{\mathbb{S}^{n-1}}(v_1, v_2) = \theta$ for some $\theta \in (0, \pi]$. Let $\psi_1, \psi_2 \in [0, \pi]$ such that $\psi_1 + \psi_2 < \theta < \pi - (\psi_1 + \psi_2)$. Then

$$\mathcal{C}^\leq(c, v_1, \psi_1) \cap \mathcal{C}^\leq(c, v_2, \psi_2) = \{c\}.$$

Finally, we consider in this paper hybrid dynamical systems [16], described through constrained differential and differ-

ence inclusions for state $X \in \mathbb{R}^n$:

$$\begin{cases} \dot{X} \in \mathbf{F}(X), & X \in \mathcal{F}, \\ X^+ \in \mathbf{J}(X), & X \in \mathcal{J}. \end{cases} \quad (15)$$

The data of the hybrid system (15) (i.e., the flow set $\mathcal{F} \subset \mathbb{R}^n$, the flow map $\mathbf{F} : \mathbb{R}^n \rightrightarrows \mathbb{R}^n$, the jump set $\mathcal{J} \subset \mathbb{R}^n$, the jump map $\mathbf{J} : \mathbb{R}^n \rightrightarrows \mathbb{R}^n$) is denoted by $\mathcal{H} = (\mathcal{F}, \mathbf{F}, \mathcal{J}, \mathbf{J})$.

III. PROBLEM FORMULATION

We consider a vehicle moving in the n -dimensional Euclidean space according to the single integrator dynamics:

$$\dot{x} = u \quad (16)$$

where $x \in \mathbb{R}^n$ is the state of the vehicle and $u \in \mathbb{R}^n$ is the control input. We assume that in the workspace there exists an obstacle considered as a spherical region $\mathcal{B}_\epsilon(c)$ centered at $c \in \mathbb{R}^n$ and with radius $\epsilon > 0$. The vehicle needs to avoid the obstacle while stabilizing its position to a given reference. Without loss of generality, we consider $n \geq 2$ ¹ and take our reference position at $x = 0$ (the origin).

Assumption 1: $\|c\| > \epsilon > 0$.

Assumption 1 requires that the reference position $x = 0$ is not inside the obstacle region, otherwise the following control objective would not be feasible. Our objective is indeed to design a control strategy for the input u such that:

- i) the obstacle-free region $\mathbb{R}^n \setminus \mathcal{B}_\epsilon(c)$ is forward invariant;
- ii) the origin $x = 0$ is globally asymptotically stable;
- iii) for each $\epsilon' > \epsilon$, there exist controller parameters such that the control law matches, in $\mathbb{R}^n \setminus \mathcal{B}_{\epsilon'}(c)$, the law $u = -k_0 x$ ($k_0 > 0$) used in the absence of the obstacle.

Objective i) guarantees that all solutions of the closed-loop system are safely avoiding the obstacle by remaining outside the obstacle region. Objectives i) and ii), together, can not be achieved using a continuous feedback due to the topological obstruction discussed in the introduction. Objective iii) is the so-called *semiglobal preservation* property [13]. This property is desirable when the original controller parameters are optimally tuned and the controller modifications imposed by the presence of the obstacle should be as minimal as possible. Such a property is also accounted for in the quadratic programming formulation of [17, III.A.]. The obstacle avoidance problem described above is solved via a hybrid feedback strategy in Sections IV-V.

IV. PROPOSED HYBRID CONTROL ALGORITHM FOR OBSTACLE AVOIDANCE

In this section, we propose a hybrid controller that switches suitably between an *avoidance* controller and a *stabilizing* controller. Let $m \in \{-1, 0, 1\}$ be a discrete variable dictating the control mode where $m = 0$ corresponds to the activation of the stabilizing controller and $|m| = 1$ corresponds to the activation of the avoidance controller, which has two configurations $m \in \{-1, 1\}$. The proposed

¹ For $n = 1$ (i.e., the state space is a line), global asymptotic stabilization with obstacle avoidance is infeasible.

control input, depending on both the state $x \in \mathbb{R}^n$ and the control mode $m \in \{-1, 0, 1\}$, is given by the feedback law

$$u = \kappa(x, m) := \begin{cases} -k_0 x, & m = 0 \\ -k_m \pi^\perp(x - c)(x - p_m), & m \in \{-1, 1\} \end{cases} \quad (17)$$

where $k_m > 0$ (with $m \in \{-1, 0, 1\}$) and $p_m \in \mathbb{R}^n$ (with $m \in \{-1, 1\}$, see (18) below) are design parameters. During the stabilization mode ($m = 0$), the control input in (17) steers x towards $x = 0$. During the avoidance mode ($|m| = 1$), the control input in (17) minimizes the distance to the *auxiliary* attractive point p_m while maintaining a constant distance to the center of the ball $\mathcal{B}_\epsilon(c)$, thereby avoiding to hit the obstacle. This is done by projecting the feedback $-k_m(x - p_m)$ on the hyperplane orthogonal to $(x - c)$. This control strategy resembles the well-known path planning Bug algorithms (see, e.g., [18]) where the motion planner switches between motion-to-goal and boundary-following objectives.

For the sets we now introduce, the reader is referred to Fig. 2 for the rest of the section. For $\theta > 0$ (further bounded in (22)), the points p_1, p_{-1} are selected to lie on the cone² $\mathcal{C}_{\leq}^\pm(c, c, \theta) \setminus \{c\}$:

$$p_1 \in \mathcal{C}_{\leq}^\pm(c, c, \theta) \setminus \{c\} \text{ and } p_{-1} := -\rho^\perp(c)p_1. \quad (18)$$

Note that, by (18), p_{-1} opposes p_1 diametrically with respect to the axis of the cone $\mathcal{C}_{\leq}^\pm(c, c, \theta)$ and also belongs to $\mathcal{C}_{\leq}^\pm(c, c, \theta) \setminus \{c\}$ as per the next lemma.

Lemma 2 ([15]): $p_{-1} \in \mathcal{C}_{\leq}^\pm(c, c, \theta) \setminus \{c\}$.

The logic variable m is selected according to a hybrid mechanism that exploits a suitable construction of the flow and jump sets. This hybrid selection is obtained through the hybrid dynamical system

$$\begin{cases} \dot{x} = \kappa(x, m) \\ \dot{m} = 0 \end{cases} \quad (x, m) \in \bigcup_{m \in \{-1, 0, 1\}} \mathcal{F}_m \times \{m\} \quad (19a)$$

$$\begin{cases} x^+ = x \\ m^+ \in \mathbf{M}(x, m) \end{cases} \quad (x, m) \in \bigcup_{m \in \{-1, 0, 1\}} \mathcal{J}_m \times \{m\}. \quad (19b)$$

The flow and jump sets for each mode $m \in \{-1, 0, 1\}$ are defined as (see (14) for the definition of the helmet \mathcal{H}):

$$\mathcal{J}_0 := \mathcal{H}(c, \epsilon, \epsilon_s, 1/2), \quad (19c)$$

$$\mathcal{F}_0 := \mathbb{R}^n \setminus (\mathcal{J}_0 \cup \mathcal{B}_\epsilon(c)), \quad (19d)$$

$$\mathcal{F}_m := \mathcal{H}(c, \epsilon, \epsilon_h, \mu) \cap \mathcal{C}_{\leq}^\pm(c, p_m - c, \psi), \quad |m| = 1, \quad (19e)$$

$$\mathcal{J}_m := \mathbb{R}^n \setminus (\mathcal{F}_m \cup \mathcal{B}_\epsilon(c)), \quad |m| = 1, \quad (19f)$$

see Fig. 2. The (set-valued) jump map is defined as

$$\mathbf{M}(x, 0) := \{m' \in \{-1, 1\} : x \in \mathcal{C}_{\leq}^\pm(c, p_{m'} - c, \bar{\psi})\} \quad (19g)$$

$$\mathbf{M}(x, m) := \{0\}, \quad \text{for } |m| = 1, \quad (19h)$$

where $\epsilon_s, \epsilon_h, \mu, \psi, \bar{\psi}, \theta$ are design parameters selected later

²Following the remark in Footnote 1, note that the set $\mathcal{C}_{\leq}^\pm(c, c, \theta) \setminus \{c\}$ is nonempty for all $n \geq 2$.

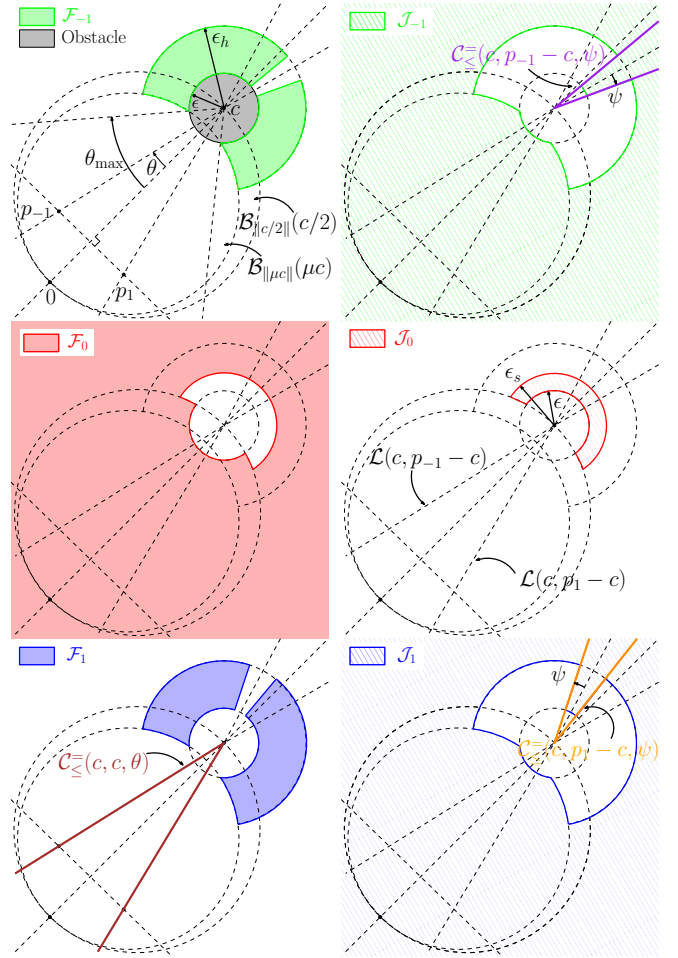


Fig. 2. 2D illustration of flow and jump sets considered in Sections IV-V.

as in Assumption 2. Before we state our main result, we motivate the above construction of flow and jump sets.

During the stabilization mode $m = 0$, the closed-loop system should not flow when x is close enough to the surface of the obstacle region $\mathcal{B}_\epsilon(c)$ and the vector field $-k_0 x$ points inside $\mathcal{B}_\epsilon(c)$. Indeed, by computing the derivative of $\|x - c\|^2$ along solutions to $\dot{x} = -k_0 x$, we can obtain the set where the stabilizing vector field $-k_0 x$ causes a decrease in the distance $\|x - c\|^2$ to the centre of the obstacle region $\mathcal{B}_\epsilon(c)$. This set is characterized by the inequality

$$-k_0 x^\top (x - c) \leq 0 \iff \|x - c/2\|^2 \geq \|c/2\|^2. \quad (20)$$

The closed set in (20) corresponds to the region outside the ball $\mathcal{B}_{\|c/2\|}(c/2)$. Therefore, to keep the vehicle safe during the stabilization mode, we define around the obstacle the helmet region $\mathcal{H}(c, \epsilon, \epsilon_s, 1/2)$ used as the jump set \mathcal{J}_0 in (19c). In other words, if during the stabilization mode the vehicle hits this *safety helmet*, then the controller jumps to avoidance mode. The amount $\epsilon_s - \epsilon$ represents the thickness of the safety helmet defining the jump set \mathcal{J}_0 .

During the avoidance mode $|m| = 1$, we want our controller to slide in the helmet $\mathcal{H}(c, \epsilon, \epsilon_h, \mu)$ while maintaining a constant distance to the center c . Note that, with $\epsilon_h > \epsilon_s$

and $\mu < 1/2$, the helmet $\mathcal{H}(c, \epsilon, \epsilon_h, \mu)$ (see also Fig. 1) is an *inflated* version of the helmet $\mathcal{H}(c, \epsilon, \epsilon_s, 1/2)$ and creates a hysteresis region useful to prevent infinitely many consecutive jumps (Zeno behavior). Let us then characterize in the next lemma the equilibria of the avoidance vector field $\kappa(x, m) = -k_m \pi^\perp(x - c)(x - p_m)$, $|m| = 1$.

Lemma 3 ([15]): For each $x \in \mathbb{R}^n \setminus \{c\}$ and $m \in \{-1, 1\}$, $\pi^\perp(x - c)(x - p_m) = 0$ if and only if $x \in \mathcal{L}(c, p_m - c)$.

Since we want the solutions to leave the set \mathcal{F}_m during the avoidance mode, it is necessary to select the point p_m and the flow set \mathcal{F}_m such that $\mathcal{L}(c, p_m - c) \cap \mathcal{F}_m = \emptyset$ for each $m \in \{-1, 1\}$, otherwise solutions can stay in the avoidance mode indefinitely. This motivates both the intersection with the conic region in (19e) and Lemma 4, in view of which we pose the next assumption.

Assumption 2: The parameters in (19) are selected as:

$$\epsilon_h \in (\epsilon, \sqrt{\epsilon \|c\|}) \quad \epsilon_s \in (\epsilon, \epsilon_h) \quad \mu \in (\mu_{\min}, 1/2) \quad (21)$$

$$\theta \in (0, \theta_{\max}) \quad \psi \in (0, \psi_{\max}) \quad \bar{\psi} \in (\psi, \psi_{\max}) \quad (22)$$

where μ_{\min} , θ_{\max} and ψ_{\max} are defined as

$$\mu_{\min} := \frac{1}{2} \frac{\epsilon_h^2 + \|c\|^2 - 2\epsilon \|c\|}{\|c\|^2 - \epsilon \|c\|} \in (0, 1/2), \quad (23)$$

$$\theta_{\max} := \arccos \left(\frac{\epsilon_h^2 + \|c\|^2 (1 - 2\mu)}{2\epsilon \|c\| (1 - \mu)} \right) \in (0, \pi/2), \quad (24)$$

$$\psi_{\max} := \min(\theta, \pi/2 - \theta) \in (0, \pi/4). \quad (25)$$

The intervals in (21)–(25) are well defined. They can be checked in this order. The intervals of ϵ_h and ϵ_s are well defined by Assumption 1. Then, those of μ_{\min} , μ , θ_{\max} ($\theta_{\max} > 0$ directly from $\mu > \mu_{\min}$), θ , ψ_{\max} and, finally, those of ψ and $\bar{\psi}$ (equivalent to $0 < \psi < \bar{\psi} < \psi_{\max}$) are also well defined.

Lemma 4 ([15]): Under Assumption 2, $\mathcal{F}_m \cap \mathcal{L}(c, p_m - c) = \emptyset$, for $m \in \{-1, 1\}$.

V. MAIN RESULT

In this section, we state and prove our main result, which corresponds to the objectives discussed in Section III. We first write compactly the flow/jump sets and maps of (19):

$$\mathcal{F} := \bigcup_{m \in \{-1, 0, 1\}} \mathcal{F}_m \times \{m\}, \quad \mathcal{J} := \bigcup_{m \in \{-1, 0, 1\}} \mathcal{J}_m \times \{m\} \quad (26)$$

$$(x, m) \mapsto \mathbf{F}(x, m) := (\kappa(x, m), 0), \quad (27)$$

$$(x, m) \mapsto \mathbf{J}(x, m) := (x, \mathbf{M}(x, m)). \quad (28)$$

The mild regularity conditions satisfied by the hybrid system (19), as in the next lemma, guarantee the applicability of many results in the proof of our main result.

Lemma 5 ([15]): The hybrid system $(\mathcal{F}, \mathbf{F}, \mathcal{J}, \mathbf{J})$ satisfies the hybrid basic conditions in [16, Ass. 6.5].

Let us define the obstacle-free set \mathcal{K} and the attractor \mathcal{A} as:

$$\mathcal{K} := \overline{\mathbb{R}^n \setminus \mathcal{B}_\epsilon(c)} \times \{-1, 0, 1\}, \quad \mathcal{A} := \{0\} \times \{0\}. \quad (29)$$

Our main result is given in the next theorem.

Theorem 1: Consider the hybrid system (19) under Assumptions 1-2. Then,

| Set to which x belongs | $\mathbf{T}_{\mathcal{F}_0}(x)$ |
|--|--|
| $\partial \mathcal{B}_\epsilon(c) \cap \mathcal{B}_{\ c/2\ }^\circ(c/2)$ | $\mathcal{P}^\geq(0, x - c)$ |
| $\partial \mathcal{B}_{\epsilon_s}(c) \setminus \mathcal{B}_{\ c/2\ }^\circ(c/2)$ | $\mathcal{P}^\geq(0, x - c)$ |
| $(\partial \mathcal{B}_{\ c/2\ }^\circ(c/2) \cap \mathcal{B}_{\epsilon_s}^\circ(c)) \setminus \mathcal{B}_\epsilon(c)$ | $\mathcal{P}^\leq(0, x - c/2)$ |
| $\partial \mathcal{B}_\epsilon(c) \cap \partial \mathcal{B}_{\ c/2\ }^\circ(c/2)$ | $\mathcal{P}^\geq(0, x - c) \cap \mathcal{P}^\leq(0, x - c/2)$ |
| $\partial \mathcal{B}_{\ c/2\ }^\circ(c/2) \cap \partial \mathcal{B}_{\epsilon_s}(c)$ | $\mathcal{P}^\geq(0, x - c) \cup \mathcal{P}^\leq(0, x - c/2)$ |

| Set to which x belongs | $\mathbf{T}_{\mathcal{F}_m}(x)$ |
|---|--|
| $\partial \mathcal{B}_\epsilon(c) \setminus \mathcal{B}_{\ c\ }(\mu c) \setminus \mathcal{C}_{\leq}^\leq(c, p_m - c, \psi)$ | $\mathcal{P}^\geq(0, x - c)$ |
| $\partial \mathcal{B}_{\epsilon_h}(c) \setminus \mathcal{B}_{\ c\ }(\mu c) \setminus \mathcal{C}_{\leq}^\leq(c, p_m - c, \psi)$ | $\mathcal{P}^\leq(0, x - c)$ |
| $\partial \mathcal{B}_{\ c\ }(\mu c) \cap \mathcal{B}_{\epsilon_h}^\circ(c) \setminus \mathcal{B}_\epsilon(c)$ | $\mathcal{P}^\geq(0, x - \mu c)$ |
| $\mathcal{C}_{\leq}^\leq(c, p_m - c, \psi) \cap \mathcal{B}_{\epsilon_h}^\circ(c) \setminus \mathcal{B}_\epsilon(c)$ | $\mathcal{P}^\geq(0, n_m(x))$ |
| $\partial \mathcal{B}_\epsilon(c) \cap \partial \mathcal{B}_{\ c\ }(\mu c)$ | $\mathcal{P}^\geq(0, x - c) \cap \mathcal{P}^\geq(0, x - \mu c)$ |
| $\partial \mathcal{B}_{\epsilon_h}(c) \cap \partial \mathcal{B}_{\ c\ }(\mu c)$ | $\mathcal{P}^\leq(0, x - c) \cap \mathcal{P}^\geq(0, x - \mu c)$ |
| $\partial \mathcal{B}_\epsilon(c) \cap \mathcal{C}_{\leq}^\leq(c, p_m - c, \psi)$ | $\mathcal{P}^\geq(0, x - c) \cap \mathcal{P}^\geq(0, n_m(x))$ |
| $\partial \mathcal{B}_{\epsilon_h}(c) \cap \mathcal{C}_{\leq}^\leq(c, p_m - c, \psi)$ | $\mathcal{P}^\leq(0, x - c) \cap \mathcal{P}^\geq(0, n_m(x))$ |

TABLE I

TANGENT CONES TO \mathcal{F}_0 AND \mathcal{F}_m AT x , WITH m EITHER -1 OR 1

$$(n_m(x) := \pi^\psi(p_m - c)(x - c)).$$

- i) all maximal solutions do not have finite escape times, are complete in the ordinary time direction, and the obstacle-free set \mathcal{K} in (29) is forward invariant (as in [19, Def. 3.3]);
- ii) the set \mathcal{A} in (29) is globally asymptotically stable;
- iii) for each $\epsilon' > \epsilon$, it is possible to tune the hybrid controller parameters so that the resulting hybrid feedback law matches, in $\mathbb{R}^n \setminus \mathcal{B}_{\epsilon'}(c)$, the law $u = -k_0 x$.

Theorem 1 shows that the three objectives discussed in Section III are fulfilled.

A. Proof of Theorem 1

To prove item i), we resort to [19, Thm. 4.3]. We first establish for \mathcal{H} in (19) the relationships invoked in [19, Thm. 4.3], and we refer the reader to Fig. 2 for a two-dimensional visualization. In particular, the boundaries of the flow sets \mathcal{F}_0 and \mathcal{F}_m , $m \in \{-1, 1\}$, are

$$\partial \mathcal{F}_0 = (\partial \mathcal{B}_\epsilon(c) \cap \mathcal{B}_{\|c/2\|}^\circ(c/2)) \cup (\partial \mathcal{B}_{\epsilon_s}(c) \setminus \mathcal{B}_{\|c/2\|}^\circ(c/2)) \cup ((\partial \mathcal{B}_{\|c/2\|}^\circ(c/2) \cap \mathcal{B}_{\epsilon_s}(c)) \setminus \mathcal{B}_\epsilon(c)), \quad (30)$$

$$\partial \mathcal{F}_m = ((\partial \mathcal{B}_\epsilon(c) \cup \partial \mathcal{B}_{\epsilon_h}(c)) \setminus \mathcal{B}_{\|c\|}(\mu c) \setminus \mathcal{C}_{\leq}^\leq(c, p_m - c, \psi)) \cup ((\partial \mathcal{B}_{\|c\|}(\mu c) \cup \mathcal{C}_{\leq}^\leq(c, p_m - c, \psi)) \cap \mathcal{B}_{\epsilon_h}(c) \setminus \mathcal{B}_\epsilon(c)). \quad (31)$$

The tangent cone (see [16, Def. 5.12 and Fig. 5.4]), evaluated at the boundary of these sets, is given in Table I.

Consider $m = 0$ and let $z := \kappa(x, 0) = -k_0 x$. If $x \in \partial \mathcal{B}_\epsilon(c) \cap \mathcal{B}_{\|c/2\|}^\circ(c/2)$, then $(x - c)^\top z = -k_0 x^\top (x - c) > 0$ (since $x \in \mathcal{B}_{\|c/2\|}^\circ(c/2)$, see (20)), i.e., $z \in \mathcal{P}^>(0, x - c)$. If $x \in (\partial \mathcal{B}_{\|c/2\|}^\circ(c/2) \cap \mathcal{B}_{\epsilon_s}(c)) \setminus \mathcal{B}_\epsilon(c)$, then one has $(x - c/2)^\top z = -k_0 x^\top (x - c/2) = -k_0 x^\top c/2 = -k_0 \|x\|^2/2 \leq 0$ since $x^\top (x - c) = 0$ from $\|x - c/2\| = \|c/2\|$. Then, $z \in \mathcal{P}^\leq(0, x - c/2)$. If $x \in \partial \mathcal{B}_\epsilon(c) \cap \partial \mathcal{B}_{\|c/2\|}^\circ(c/2)$ or $x \in \partial \mathcal{B}_{\|c/2\|}^\circ(c/2) \cap \partial \mathcal{B}_{\epsilon_s}(c)$, then $z^\top (x - c) = 0$ and $z^\top (x - c/2) = -k_0 \|x\|^2/2 \leq 0$ showing, respectively,

that $z \in \mathcal{P}^{\geq}(0, x - c) \cap \mathcal{P}^{\leq}(0, x - c/2)$. Finally, if $x \in \partial\mathcal{B}_{\epsilon_s}(c) \setminus \mathcal{B}_{\|c/2\|}(c/2)$, then $(x - c)^\top z = -k_0 x^\top (x - c) < 0$ (since $x \notin \mathcal{B}_{\|c/2\|}(c/2)$), i.e., $z \in \mathcal{P}^<(0, x - c)$. Let $\mathcal{L}_0 := \partial\mathcal{B}_{\epsilon_s}(c) \setminus \mathcal{B}_{\|c/2\|}(c/2)$. Therefore, by all the previous arguments, (30) and Table I:

$$\begin{aligned} x \in \mathcal{L}_0 &\implies \kappa(x, 0) \cap \mathbf{T}_{\mathcal{F}_0}(x) = \emptyset \\ x \in \partial\mathcal{F}_0 \setminus \mathcal{L}_0 &\implies \kappa(x, 0) \subset \mathbf{T}_{\mathcal{F}_0}(x). \end{aligned} \quad (32)$$

Consider then $m \in \{-1, 1\}$ and let now $z := \kappa(x, m) = -k_m \pi^\perp(x - c)(x - p_m)$. If $x \in \partial\mathcal{B}_\epsilon(c)$ or $x \in \partial\mathcal{B}_{\epsilon_h}(c)$ then one has $(x - c)^\top z = -k_m(x - c)^\top \pi^\perp(x - c)(x - p_m) = 0$, which implies that both $z \in \mathcal{P}^{\geq}(0, x - c)$ and $z \in \mathcal{P}^{\leq}(0, x - c)$. Define $n_m(x) := \pi^\psi(p_m - c)(x - c)$, which is a normal vector to the cone $\mathcal{C}^\pm(c, p_m - c, \psi)$ at x . If $x \in \mathcal{C}_\leq^\pm(c, p_m - c, \psi)$, then³

$$\begin{aligned} n_m(x)^\top z &= -k_m n_m(x)^\top \pi^\perp(x - c)(x - p_m) \\ &\stackrel{(3)}{=} k_m(x - c)^\top \pi^\psi(p_m - c) \pi^\perp(x - c)(p_m - c) \\ &\stackrel{(8),(5)}{=} k_m(x - c)^\top (\pi^\perp(p_m - c) - \sin^2(\psi) I_n) \pi^\perp(x - c)(p_m - c) \\ &\stackrel{(3)}{=} k_m(x - c)^\top \pi^\perp(p_m - c) \pi^\perp(x - c)(p_m - c) \\ &\stackrel{(5)}{=} k_m(x - c)^\top \pi^\perp(p_m - c) (I_n - \pi^\parallel(x - c))(p_m - c) \\ &\stackrel{(3)}{=} -k_m(x - c)^\top \pi^\perp(p_m - c) \pi^\parallel(x - c)(p_m - c) \\ &\stackrel{(1)}{=} -k_m \frac{(x - c)^\top \pi^\perp(p_m - c)(x - c)}{\|x - c\|^2} (x - c)^\top (p_m - c) \geq 0 \end{aligned}$$

where the last bound follows from $\pi^\perp(p_m - c)$ positive semidefinite and $(x - c)^\top (p_m - c) \leq 0$ (since $x \in \mathcal{C}_\leq^\pm(c, p_m - c, \psi) \subset \mathcal{P}^{\leq}(c, p_m - c)$). Hence, $z \in \mathcal{P}^{\geq}(0, n_m(x))$. Finally, let $x \in \partial\mathcal{B}_{\|\mu c\|}(\mu c) \cap \mathcal{B}_{\epsilon_h}(c) \setminus \mathcal{B}_\epsilon(c)$. With θ_{\max} in (24) and $\mu < 1/2$, we have

$$\begin{aligned} 0 \leq c^\top (c - x) &= \frac{\|x - c\|^2 + (1 - \mu)^2 \|c\|^2 - \|x - \mu c\|^2}{2(1 - \mu)} \\ &= \frac{\|x - c\|^2 + \|c\|^2(1 - 2\mu)}{2(1 - \mu)} \leq \frac{\epsilon_h^2 + \|c\|^2(1 - 2\mu)}{2(1 - \mu)} \quad (33) \\ &= \cos(\theta_{\max}) \epsilon \|c\| \leq \cos(\theta_{\max}) \|x - c\| \|c\|. \end{aligned}$$

From $c^\top (p_m - c) = -\cos(\theta) \|c\| \|p_m - c\|$ ($p_m \in \mathcal{C}_\leq^\pm(c, c, \theta)$ by (18) and Lemma 2) and (33), we get the first bound in

$$\begin{aligned} (x - \mu c)^\top z &= -k_m(x - \mu c)^\top \pi^\perp(x - c)(x - p_m) \\ &\stackrel{(3)}{=} k_m(c - \mu c)^\top \pi^\perp(x - c)(p_m - c) \\ &\stackrel{(1)}{=} k_m(1 - \mu)(c^\top (p_m - c) \\ &\quad + c^\top (c - x) \cdot (x - c)^\top (p_m - c) / \|x - c\|^2) \\ &\leq k_m(1 - \mu)(-\cos(\theta) + \cos(\theta_{\max})) \|c\| \|p_m - c\| < 0, \end{aligned}$$

and $k_m > 0$, $1 - \mu > 0$ (from (21)), $\theta < \theta_{\max}$ (from (22)) yield the second bound. $(x - \mu c)^\top z < 0$ implies then $z \in \mathcal{P}^<(0, x - \mu c)$. Let $\mathcal{L}_m := \partial\mathcal{B}_{\|\mu c\|}(\mu c) \cap \mathcal{B}_{\epsilon_h}(c) \setminus \mathcal{B}_\epsilon(c)$. Therefore, by all the previous arguments, (31) and Table I:

$$\begin{aligned} x \in \mathcal{L}_m &\implies \kappa(x, m) \cap \mathbf{T}_{\mathcal{F}_m}(x) = \emptyset \\ x \in \partial\mathcal{F}_m \setminus \mathcal{L}_m &\implies \kappa(x, m) \subset \mathbf{T}_{\mathcal{F}_m}(x). \end{aligned} \quad (34)$$

³Each (in)equality is obtained thanks to the relationship reported over it.

We can now apply [19, Thm. 4.3]. With \mathcal{K} in (29), let $\hat{\mathcal{F}} := \partial(\mathcal{K} \cap \mathcal{F}) \setminus \mathcal{L}$ with $\mathcal{L} = \cup_{m=-1,0,1} \mathcal{L}_m \times \{m\}$. By (32) and (34) and $\mathcal{K} \cap \mathcal{F} = \mathcal{F}$, we have $\hat{\mathcal{F}} = \cup_{m=-1,0,1} (\partial\mathcal{F}_m \setminus \mathcal{L}_m) \times \{m\}$. It follows from (32) and (34) that for every $(x, m) \in \hat{\mathcal{F}}$, $\mathbf{F}(x, m) \subset \mathbf{T}_{\mathcal{F}}(x, m)$. Also, $\mathbf{J}(\mathcal{K} \cap \mathcal{F}) \subset \mathcal{K}$, \mathcal{F} is closed, the map \mathbf{F} satisfies the hybrid basic conditions as proven in Lemma 5 and it is, moreover, locally Lipschitz since it is continuously differentiable. We conclude then that the set \mathcal{K} is forward pre-invariant [19, Def. 3.3]. In addition, since $\mathcal{L}_0 \subset \mathcal{J}_0$ and $\mathcal{L}_m \subset \mathcal{J}_m$ with $m \in \{-1, 1\}$, one has $\mathcal{L} \subset \mathcal{J}$. Besides, finite escape times can only occur through flow, and since the sets \mathcal{F}_{-1} and \mathcal{F}_1 are bounded by their definitions in (19e), finite escape times cannot occur for $x \in \mathcal{F}_{-1} \cup \mathcal{F}_1$. They can neither occur for $x \in \mathcal{F}_0$ because they would make $x^\top x$ grow unbounded, and this would contradict that $\frac{d}{dt}(x^\top x) \leq 0$ by the definition of $\kappa(x, 0)$ and by (19a). Therefore, all maximal solutions do not have finite escape times. By [19, Thm. 4.3] again, the set \mathcal{K} is actually forward invariant [19, Def. 3.3], and solutions are complete. Finally, we anticipate here an immediate corollary of completeness of solutions and Lemma 6 below: since the number of jumps is finite by Lemma 6, all maximal solutions to (19) are actually complete in the ordinary time direction.

To prove item ii), we proceed in two steps. First, we prove that the set \mathcal{A} is globally asymptotically stable for the system without jumps. To this end, the *jumpless system* has data $\mathcal{H}^0 = (\mathbf{F}, \mathcal{F}, \emptyset, \emptyset)$ with flow map \mathbf{F} and flow set \mathcal{F} defined in (19). We emphasize that \mathcal{H}^0 is obtained in accordance to [20, Eqs. (38)-(39)] by identifying *all* jumps with events. Consider the Lyapunov function

$$\mathbf{V}(x, m) := m^2/2 + \|x - p_m\|^2/2, \quad (35)$$

with $p_0 := 0$ and p_m ($m \in \{-1, 1\}$) defined in (18). One has $\mathbf{V}(x, m) = 0$ for all $(x, m) \in \mathcal{A}$ in (29), $\mathbf{V}(x, m) > 0$ for all $(x, m) \notin \mathcal{A}$, and is radially unbounded relative to $\mathcal{F} \cup \mathcal{J}$. Straightforward computations show that

$$\begin{aligned} \langle \nabla \mathbf{V}(x, 0), \mathbf{F}(x, 0) \rangle &= -k_0 x^\top x < 0 \quad \forall x \in \mathcal{F}_0 \setminus \{0\} \\ \langle \nabla \mathbf{V}(x, m), \mathbf{F}(x, m) \rangle &= -k_m(x - p_m)^\top \pi^\perp(x - c)(x - p_m) \\ &= -k_m \|\pi^\perp(x - c)(x - p_m)\|^2 < 0 \quad \forall m \in \{-1, 1\}, x \in \mathcal{F}_m. \end{aligned}$$

The last inequality follows from projection matrices being positive semidefinite and Lemma 3, which implies that it cannot be $\langle \nabla \mathbf{V}(x, m), \mathbf{F}(x, m) \rangle = 0$ for $m \in \{-1, 1\}$ and all $x \in \mathcal{F}_m$ since $\mathcal{L}(c, p_m - c)$ is excluded from \mathcal{F}_m by Lemma 4. All the above conditions satisfied by \mathbf{V} suffice to conclude global asymptotic stability of \mathcal{A} for \mathcal{H}^0 since \mathcal{A} is compact and \mathcal{H}^0 satisfies [16, Ass. 6.5].

Second, the next lemma establishes that the number of jumps is finite for the given hybrid dynamics in (19).

Lemma 6 ([15]): For \mathcal{H} in (19), each solution starting in \mathcal{K} experiences no more than 3 jumps.

Consequently, global asymptotic stability of \mathcal{A} follows from the first and second step by [20, Thm. 31], since the hybrid system in (19) satisfies the Basic Assumptions [20, p. 43], as proven in Lemma 5, the set \mathcal{A} is compact and has empty intersection with the jump set.

Lastly, to prove item iii), let $\epsilon' > \epsilon$. Select the parameter $\epsilon_h \in (\epsilon, \min(\epsilon', \sqrt{\epsilon\|c\|}))$ while all other hybrid controller parameters are selected as in Assumption 2. Then this implies that the flow sets $\mathcal{F}_m, m \in \{-1, 1\}$, of the avoidance mode are entirely contained in $\mathcal{B}_{\epsilon'}(c)$. Therefore, as long as the state x remains in $\mathbb{R}^n \setminus \mathcal{B}_{\epsilon'}(c)$, solutions are enforced to flow only with the stabilizing mode $m = 0$, which corresponds to the feedback law $u = -k_0x$.

VI. NUMERICAL EXAMPLE

We illustrate our results through a three-dimensional example. The hybrid system in (19) is fully specified by the following parameters. The obstacle has center $c = (1, 1, 1)$ and radius $\epsilon = 0.700$. The controller gains are $k_m = 1$ for $m \in \{-1, 0, 1\}$. The parameters used in the construction of the flow and jump sets are $\epsilon_h = 0.901$, $\epsilon_s = 0.800$, $\mu = 0.444$, $\theta = 0.276$, which satisfy Assumption 2. To select a point $p_1 \in \mathcal{C}_{\leq}^-(c, c, \theta) \setminus \{c\}$, we proceed as follows. Select $v \in \mathbb{S}^n$ such that $v^\top c = 0$ and consider $\mathbf{R}(v, \theta) \in \mathbb{SO}(3)$, i.e., an orthogonal rotation matrix specified by axis v and angle θ . Then, we can verify that the point $p_1 = (I_3 - \mathbf{R}(v, \theta))c$ is a point on the cone $\mathcal{C}_{\leq}^-(c, c, \theta)$. By letting $v = (0, 1, -1)$, we determine $p_1 = (0.424, -0.155, -0.155)$ and $p_{-1} = (-0.348, 0.231, 0.231)$ as in (18). We also select $\psi = 0.249$ and $\bar{\psi} = 0.266$, which satisfy Assumption 2. Fig. 3 shows that the objectives posed in Section III and proven in Theorem 1 are fulfilled. The top part of the figure illustrates the relevant sets. The middle part shows that the origin is globally asymptotically stable, and the control law matches the stabilizing one sufficiently away from the obstacle. The bottom part shows that the solutions are safe since they all stay away from the obstacle set $\mathcal{B}_\epsilon(c)$.

VII. CONCLUSIONS

We have proposed a hybrid feedback law for the avoidance of a spherical obstacle in \mathbb{R}^n . This law guarantees forward invariance of the obstacle-free space and global asymptotic stability of the reference. Future work includes generalizing this control strategy to multiple, nonspherical obstacles.

REFERENCES

- [1] O. Khatib, "Real-time obstacle avoidance for manipulators and mobile robots," in *Autonomous robot vehicles*. Springer, 1986, pp. 396–404.
- [2] D. E. Koditschek and E. Rimon, "Robot navigation functions on manifolds with boundary," *Advances in applied mathematics*, vol. 11, no. 4, pp. 412–442, 1990.
- [3] D. V. Dimarogonas, S. G. Loizou, K. J. Kyriakopoulos, and M. M. Zavlanos, "A feedback stabilization and collision avoidance scheme for multiple independent non-point agents," *Automatica*, vol. 42, no. 2, pp. 229–243, 2006.
- [4] I. Filippidis and K. J. Kyriakopoulos, "Navigation functions for focally admissible surfaces," in *Amer. Control Conf.*, 2013, pp. 994–999.
- [5] F. Wilson Jr, "The structure of the level surfaces of a Lyapunov function," *Journal of Differential Equations*, 1967.
- [6] S. G. Loizou, "The navigation transformation," *IEEE Trans. Robot.*, vol. 33, no. 6, pp. 1516–1523, 2017.
- [7] S. Prajna, A. Jadbabaie, and G. J. Pappas, "A framework for worst-case and stochastic safety verification using barrier certificates," *IEEE Trans. Automat. Contr.*, vol. 52, no. 8, pp. 1415–1428, 2007.
- [8] P. Wieland and F. Allgöwer, "Constructive safety using control barrier functions," *IFAC Proceedings*, vol. 40, no. 12, pp. 462–467, 2007.
- [9] M. Z. Romdony and B. Jayawardhana, "Stabilization with guaranteed safety using control Lyapunov–barrier function," *Automatica*, vol. 66, pp. 39–47, 2016.

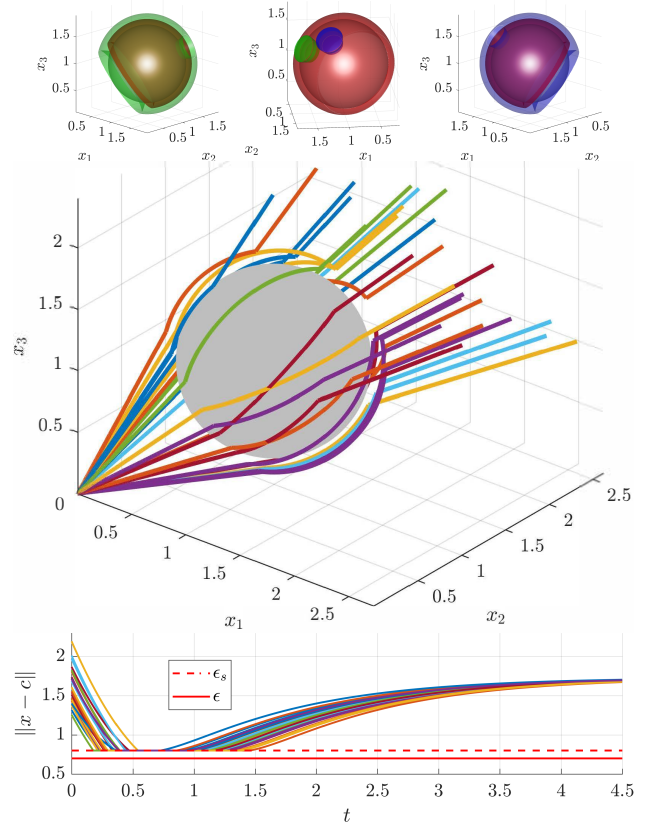


Fig. 3. Top left: sets \mathcal{F}_{-1} (green) and \mathcal{J}_0 (red) surrounding $\mathcal{B}_\epsilon(c)$ (grey). Top center: sets \mathcal{J}_0 (red), $\mathcal{J}_{-1} \cap \mathcal{H}(c, \epsilon, \epsilon_h, \mu)$ (green), and $\mathcal{J}_1 \cap \mathcal{H}(c, \epsilon, \epsilon_h, \mu)$ (blue) surrounding $\mathcal{B}_\epsilon(c)$ (grey). Top right: \mathcal{F}_1 (blue) and \mathcal{J}_0 (red) surrounding $\mathcal{B}_\epsilon(c)$ (grey). Middle: phase portrait of solutions with different initial conditions and $\mathcal{B}_\epsilon(c)$ (grey). Bottom: distance to the obstacle for the solutions and radii ϵ_s, ϵ of $\mathcal{H}(c, \epsilon, \epsilon_s, 1/2)$, $\mathcal{B}_\epsilon(c)$.

- [10] A. D. Ames, X. Xu, J. W. Grizzle, and P. Tabuada, "Control barrier function based quadratic programs for safety critical systems," *IEEE Trans. Automat. Contr.*, vol. 62, no. 8, pp. 3861–3876, 2017.
- [11] R. G. Sanfelice, M. J. Messina, S. E. Tuna, and A. R. Teel, "Robust hybrid controllers for continuous-time systems with applications to obstacle avoidance and regulation to disconnected set of points," in *Amer. Control Conf.*, 2006, pp. 3352–3357.
- [12] J. I. Poveda, M. Benosman, A. R. Teel, and R. G. Sanfelice, "A hybrid adaptive feedback law for robust obstacle avoidance and coordination in multiple vehicle systems," in *Amer. Control Conf.*, 2018, pp. 616–621.
- [13] P. Braun, C. M. Kellett, and L. Zaccarian, "Unsafe point avoidance in linear state feedback," *IEEE Conf. on Decision and Control*, 2018.
- [14] C. D. Meyer, *Matrix analysis and applied linear algebra*. SIAM, 2000.
- [15] S. Berkane, A. Bisoffi, and D. V. Dimarogonas, "A hybrid controller for obstacle avoidance in an n-dimensional Euclidean space," arXiv:1903.04392 [cs.SY], 2019.
- [16] R. Goebel, R. G. Sanfelice, and A. R. Teel, *Hybrid Dynamical Systems: modeling, stability, and robustness*. Princeton University Press, 2012.
- [17] L. Wang, A. D. Ames, and M. Egerstedt, "Safety barrier certificates for collisions-free multirobot systems," *IEEE Trans. Robot.*, vol. 33, no. 3, pp. 661–674, 2017.
- [18] V. J. Lumelsky and T. Skewis, "Incorporating range sensing in the robot navigation function," *IEEE Trans. Syst., Man, Cybern.*, vol. 20, no. 5, pp. 1058–1069, 1990.
- [19] J. Chai and R. G. Sanfelice, "Forward invariance of sets for hybrid dynamical systems (Part I)," *IEEE Trans. Automat. Contr.*, 2019.
- [20] R. Goebel, R. G. Sanfelice, and A. R. Teel, "Hybrid dynamical systems," *IEEE Control Syst. Mag.*, vol. 29, no. 2, pp. 28–93, 2009.